CERN-TH/99-113

MAGNETIC OSCILLATIONS IN DENSE COLD QUARK MATTER WITH FOUR-FERMION INTERACTIONS

D. Ebert[*] , **K.G. Klimenko**[‡] , **M.A. Vdovichenko**[†] and **A.S. Vshivtsev**[†]

[*] *Theory Division, CERN, CH 1211 Geneva 23, Switzerland*
and Institut für Physik, Humboldt-Universität, D-10115 Berlin, Germany
e-mail: dietmar.ebert@cern.ch
[‡] *Institute for High Energy Physics, 142284 Protvino, Moscow Region, Russia*
e-mail: kklim@mx.ihep.su
[†] *Moscow Institute of Radio-Engineering, Electronics and Automatic Systems,*
117454 Moscow, Russia

ABSTRACT

The phase structures of Nambu–Jona-Lasinio models with one or two flavours have been investigated at non-zero values of μ and H, where H is an external magnetic field and μ is the chemical potential. In the phase portraits of both models there arise infinitely many massless chirally symmetric phases, as well as massive ones with spontaneously broken chiral invariance, reflecting the existence of infinitely many Landau levels. Phase transitions of first and second orders and a lot of tricritical points have been shown to exist in phase diagrams. In the massless case, such a phase structure leads unavoidably to the standard van Alphen–de Haas magnetic oscillations of some thermodynamical quantities, including magnetization, pressure and particle density. In the massive case we have found an oscillating behaviour not only for thermodynamical quantities, but also for a dynamical quantity as the quark mass. Besides, in this case we have non-standard, i.e. non-periodic, magnetic oscillations, since the frequency of oscillations is an H-dependent quantity.

CERN-TH/99-113
April 1999

1. Introduction

The exploration of strongly interacting matter at high density and in the presence of external electromagnetic fields is of fundamental interest and has potential applications to the quark–gluon plasma and heavy-ion collisions, to cosmology and astrophysics of neutron stars. Recently, some aspects of this problem were considered in [1], where it was pointed out that in QCD at high density a new phase with colour superconductivity might exist. The influence of external magnetic fields on the QCD vacuum was, for example, studied in [2].

Our goal is to investigate properties of the strongly interacting cold quark matter in the presence of both external magnetic field H and non-zero chemical potential μ. The subject is closely related to magnetic oscillations of different physical quantities. In this connection we should remember that the van Alphen–de Haas effect (oscillations of the magnetization) was for the first time predicted by Landau and then experimentally observed in some non-relativistic systems (in metals) more than sixty years ago [3, 4]. At present, a lot of the attention of researchers dealing with magnetic oscillations is focused on relativistic condensed matter systems (mainly on QED at $\mu, H \neq 0$), since the results of these studies may be applied to cosmology, astrophysics and high-energy physics [5, 6].

It is well known that up to now the consideration of QCD at $\mu, H \neq 0$ is a difficult problem. This is partly due to the fact that numerical lattice simulations at $\mu \neq 0$ have not been able to overcome problems associated with the complex part of the fermionic determinant. Moreover, the incorporation of a magnetic field into lattice gauge calculations is not elaborated sufficiently, either. For these reasons, when considering quark matter at $\mu, H \neq 0$, many authors prefer to deal with adequate models (e.g. with the MIT bag model [7]), rather than with QCD.

In the present paper we shall study the above problem in the framework of some specific QCD-like quark models. Namely, we shall investigate the influence of an external magnetic field and chemical potential on the vacuum structure of Nambu–Jona-Lasinio (NJL) models containing four-fermion interactions [8, 9]. The simplest one, denoted as model I, refers to the one-flavour case and is presented by the Lagrangian

$$L_1 = \bar{q}_k i\hat{\partial} q_k + \frac{G}{2N_c}[(\bar{q}_k q_k)^2 + (\bar{q}_k i\gamma_5 q_k)^2], \tag{1}$$

where all quark fields belong to the fundamental multiplet of the colour $SU(N_c)$ group (here the summation over the colour index $k = 1, ..., N_c$ is implied). Obviously, L_1 is invariant under (global) $SU(N_c)$ and $U(1)_V$ transformations as well as continuous $U(1)_A$ chiral transformations

$$q_k \to e^{i\theta\gamma_5} q_k \quad ; \quad (k = 1, ..., N_c). \tag{2}$$

The second, more realistic case considered here and referred to as model II is a two-flavour NJL model whose Lagrangian has the form

$$L_2 \;\; = \;\; \bar{q} i\hat{\partial} q + \frac{G}{2N_c}[(\bar{q}q)^2 + (\bar{q} i\gamma^5 \vec{\tau} q)^2], \tag{3}$$

where q is a flavour isodoublet and colour-N_c-plet quark field and $\vec{\tau}$ are isospin Pauli matrices (in (3) and below, flavour and colour indices of the quark field q are now suppressed). The Lagrangian L_2 is invariant under (global) $U(2)_f \times SU(N_c)$ as well as under chiral $U(2)_L \times U(2)_R$ groups.

NJL models were proposed as a good laboratory for investigating the non-perturbative phenomenon of dynamical chiral symmetry breaking (DCSB), which occurs in the physics of strong interactions, as well as for describing the low-energy sector of QCD (see e.g. papers [10, 11, 12] and references therein). Since there are no closed physical systems in nature, the influence of different external factors on the DCSB mechanism is of great interest. In this relation, special attention has been paid to the analysis of the vacuum structure of NJL-type models at non-zero temperature and chemical potential [13, 14], in the presence of external (chromo-)magnetic fields [15, 16, 17], with allowance for curvature and non-trivial space-time topology [18, 19]. The combined influence of external electromagnetic and gravitational fields on the DCSB effect in four-fermion field theories was investigated in [20, 21].

In the present paper the phase structures and related oscillating effects of the above-mentioned Nambu– Jona-Lasinio models are considered at $\mu, H \neq 0$. We will show that, here, the set of oscillating physical parameters in NJL models is richer than in QED at $\mu, H \neq 0$. Besides, in the NJL models, in contrast to QED and similar to some condensed- matter materials, there exist non-periodic magnetic oscillations.

2. NJL models at $\mu \neq 0$ and $H = 0$

First of all let us prepare the basis for the investigations in the following sections and consider in detail the phase structure of the model I at non-zero chemical potential $\mu \neq 0$ and $H = 0$.

Recall some well-known vacuum properties of the theory (1) at $\mu = 0$. The introduction of an intermediate quark–meson Lagrangian

$$\tilde{L}_1 = \bar{q} i\hat{\partial} q - \bar{q}(\sigma_1 + i\sigma_2\gamma_5)q - \frac{N_c}{2G}(\sigma_1^2 + \sigma_2^2) \tag{4}$$

greatly facilitates the problem under consideration. (In (4) and other formulae below we have omitted the fermionic index k for simplicity.) Clearly, using the equations of motion for the bosonic fields $\sigma_{1,2}$, the theory in (4) is equivalent to that in (1). From (4) we obtain the one-loop expression for the effective action

$$\exp(iN_c S_{eff}(\sigma_{1,2})) = \int D\bar{q}Dq \exp\left(i \int \tilde{L}_1 d^4x\right),$$

where

$$S_{eff}(\sigma_{1,2}) = -\int d^4x \frac{\sigma_1^2 + \sigma_2^2}{2G} - i \ln\det(i\hat{\partial} - \sigma_1 - i\gamma_5\sigma_2).$$

Assuming that in this formula $\sigma_{1,2}$ are independent of space-time points, we have by definition

$$S_{eff}(\sigma_{1,2}) = -V_0(\sigma_{1,2}) \int d^4x,$$

$$V_0(\sigma_{1,2}) = \frac{\Sigma^2}{2G} + 2i \int \frac{d^4p}{(2\pi)^4} \ln(\Sigma^2 - p^2) \equiv V_0(\Sigma), \tag{5}$$

where $\Sigma = \sqrt{\sigma_1^2 + \sigma_2^2}$. Next, introducing in (5) Euclidean metric ($p_0 \to ip_0$) and cutting off the range of integration ($p^2 \leq \Lambda^2$), we obtain

$$V_0(\Sigma) = \frac{\Sigma^2}{2G} - \frac{1}{16\pi^2}\left\{\Lambda^4 \ln\left(1 + \frac{\Sigma^2}{\Lambda^2}\right) + \Lambda^2\Sigma^2 - \Sigma^4 \ln\left(1 + \frac{\Lambda^2}{\Sigma^2}\right)\right\}. \tag{6}$$

The stationarity equation for the effective potential (6) has the form

$$\frac{\partial V_0(\Sigma)}{\partial \Sigma} = 0 = \frac{\Sigma}{4\pi^2}\left\{\frac{4\pi^2}{G} - \Lambda^2 + \Sigma^2 \ln\left(1 + \frac{\Lambda^2}{\Sigma^2}\right)\right\} \equiv \frac{\Sigma}{4\pi^2} F(\Sigma). \tag{7}$$

Now one can easily see that at $G < G_c = 4\pi^2/\Lambda^2$ Eq. (7) has no solutions apart from $\Sigma = 0$. Hence, in this case fermions are massless, and chiral invariance (2) is not broken.

If $G > G_c$, then Eq. (7) has one non-trivial solution, $\Sigma_0(G, \Lambda) \neq 0$, such that $F(\Sigma_0) = 0$. In this case Σ_0 is a point of global minimum for the potential $V_0(\Sigma)$. This means that spontaneous breaking of the symmetry (2) takes place. Moreover, fermions acquire a mass $M \equiv \Sigma_0(G, \Lambda)$.

Let us now consider the case where $\mu > 0$ and the temperature $T \neq 0$. In this case, the effective potential $V_{\mu T}(\Sigma)$ can be found if the measure of integration in (5) is transformed in the standard way according to the rule [22]

$$\int \frac{dp_0}{2\pi} \to iT \sum_{n=-\infty}^{\infty}, \qquad p_0 \to i\pi T(2n+1) + \mu.$$

Summing there over n and letting the temperature in the obtained expression tend to zero, we obtain

$$V_\mu(\Sigma) = V_0(\Sigma) - 2 \int \frac{d^3p}{(2\pi)^3} \theta(\mu - \sqrt{\Sigma^2 + p^2})(\mu - \sqrt{\Sigma^2 + p^2}),$$

where $\theta(x)$ is the step function. Finally, by performing the momentum integration, we find

$$\begin{aligned} V_\mu(\Sigma) \;\; &= \;\; V_0(\Sigma) - \frac{\theta(\mu - \Sigma)}{16\pi^2}\left\{\frac{10}{3}\mu(\mu^2 - \Sigma^2)^{3/2} - \right. \\ &\left. - \; 2\mu^3\sqrt{\mu^2 - \Sigma^2} + \Sigma^4 \ln\left[(\mu + \sqrt{\mu^2 - \Sigma^2})^2/\Sigma^2\right]\right\}. \end{aligned} \tag{8}$$

It follows from (8) that, in the case $G < G_c$ and at arbitrary values of the chemical potential, the chiral symmetry (2) is not broken. However, at $G > G_c$ the model has a rich phase structure, which is presented in Fig. 1 in terms of μ and M. (At $G > G_c$ one can use the fermionic mass M as an independent parameter of the theory. The three quantities G, M and Λ are connected by Eq. (7).) In this figure the solid and dashed lines represent the critical curves of the second- and first-order phase transitions, respectively. Furthermore, there are two tricritical points [1],

[1] A point of the phase diagram is called a tricritical one if, in an arbitrarily small vicinity of it, there are first- as well as second-order phase transitions.

α and β, two massive phases B and C with spontaneously broken chiral invariance as well as the symmetric massless phase A in the phase portrait of the NJL model I (detailed calculations of the vacuum structure of this NJL model can be found in [14]). In the present model the dynamical quark mass $\Sigma_0(\mu)$, given by the global minimum of the potential $V_\mu(\Sigma)$ as a function of μ behaves as depicted in Fig. 2.

We should note that the phase transition from B to C is the quark-matter analogue of the so-called insulator–metal phase transition in condensed-matter physics. This is due to the fact that, in the vacuum of phase B, the particle density (the analogue of conductivity electron density in condensed materials) is zero, while in the vacuum of phase C there arises a non-zero density of charged particles, so that it looks like a Fermi-liquid ground state of metals.

To investigate the vacuum properties of the two-flavour NJL model (model II) it is again convenient to employ, instead of the quark Lagrangian (3), the equivalent quark–meson Lagrangian

$$\tilde{L}_2 = \bar{q}i\gamma^\mu\partial_\mu q - \bar{q}(\sigma + i\gamma^5\vec{\tau}\vec{\pi})q - \frac{N_c}{2G}(\sigma^2 + \vec{\pi}^2). \tag{9}$$

Using here calculations similar to the case with model I, one can find the effective potentials for $\mu = 0$ and $\mu \neq 0$ expressed in terms of meson fields $\sigma, \vec{\pi}$. These potentials have the form of the potentials (6) and (8) for the model I, respectively, with the exception that the factor $(16\pi^2)^{-1}$ in (6),(8) has to be replaced by $(8\pi^2)^{-1}$. Moreover [2], in the case under consideration $\Sigma^2 = \sigma^2 + \vec{\pi}^2$. It follows from this similarity that the phase structure and the phase portrait of the model II are qualitatively the same as those of the model I (see Fig. 1).

3. Phase structure of the model I at $\mu \neq 0$ and $H \neq 0$

In the present section we shall study vacuum magnetic properties of NJL systems. For the model I at $\mu = 0$, this problem was considered in [15, 17]. It was shown in [15] that at $G > G_c$ the chiral symmetry is spontaneously broken for arbitrary values of the external magnetic field H, including the case $H = 0$. At $G < G_c$ the NJL model I has a symmetric vacuum at $H = 0$. However, if an external (arbitrarily small) magnetic field is switched on, then for all $G \in (0, G_c)$ there is a spontaneous breaking of the initial $U(1)_A$ symmetry (2) [17]. This is the so-called effect of dynamical chiral-symmetry breaking (DCSB) catalysis by an external magnetic field. (This effect was observed for the first time in the framework of a (2+1)-dimensional Gross–Neveu model in [23] and was then explained in [24]. Now this effect is under intensive investigations since it has a wide range of possible applications in physics[3].)

Let us recall some aspects of the problem at $\mu = 0, H \neq 0$. In order to find in this case the effective potential $V_H(\Sigma)$ of the NJL model I, gauged by an external magnetic field according to $\partial_\mu \to D_\mu = \partial_\mu - ieA_\mu$, $A_\mu = \delta_{\mu 2}x_1 H$, one can use the well-known proper-time method [26]

[2] Chiral symmetry of the two-flavour NJL model (3) is realized in the space of meson fields $(\sigma, \vec{\pi})$ as the rotation group $O(4)$, which leaves the "length" of the particle vector $(\sigma, \vec{\pi})$ invariant. Hence, all effective potentials of this model depend on the single variable $\Sigma = \sqrt{\sigma^2 + \vec{\pi}^2}$. In the following we choose $\vec{\pi} = 0$, assuming the absence of a pion condensate.

[3] Some recent references on this subject are presented in [25].

or momentum-space calculations [27], which give the following expression:

$$V_H(\Sigma) = \frac{H^2}{2} + \frac{\Sigma^2}{2G} + \frac{eH}{8\pi^2}\int_0^\infty \frac{ds}{s^2}\exp(-s\Sigma^2)\ \coth(eHs).$$

In this formula e has a positive value. It is useful to rearrange this expression in the form

$$V_H(\Sigma) = V_0(\Sigma) + Z(\Sigma) + \tilde{V}_H(\Sigma), \tag{10}$$

where

$$\begin{aligned} V_0(\Sigma) &= \frac{\Sigma^2}{2G} + \frac{1}{8\pi^2}\int_0^\infty \frac{ds}{s^3}\exp(-s\Sigma^2), \\ Z(\Sigma) &= \frac{H^2}{2} + \frac{(eH)^2}{24\pi^2}\int_0^\infty \frac{ds}{s}\exp(-s\Sigma^2), \\ \tilde{V}_H(\Sigma) &= \frac{1}{8\pi^2}\int_0^\infty \frac{ds}{s^3}\exp(-s\Sigma^2)\left[\ (eHs)\coth(eHs) - 1 - \frac{(eHs)^2}{3}\ \right], \end{aligned} \tag{11}$$

thereby isolating the contributions of the matter, the field and the electromagnetic interaction energy densities explicitly. The potential $V_0(\Sigma)$ in (11) is up to an unimportant (infinite) additive constant not depending on Σ, equal to expression (5). Hence, the ultra-violet (UV)-regularized expression for it looks like (6).

The integral of the function $Z(\Sigma)$ is also UV-divergent, so we need to regularize it. The simplest possibility is to cut it off at the lower boundary, which yields

$$Z(\Sigma) = \frac{H^2}{2} - \frac{(eH)^2}{24\pi^2}\ (\ln\frac{\Sigma^2}{\Lambda^2} + \gamma), \tag{12}$$

γ being the Euler constant. Clearly, the last term in (12) contributes to the renormalization of the magnetic field and electric charge, in a way similar to what occurs in quantum electrodynamics [26].

The potential $\tilde{V}_H(\Sigma)$ in (11) has no UV divergences, so it is easily calculated with the help of integral tables [28]. The final expression for $V_H(\Sigma)$ in terms of renormalized quantities is then given by

$$V_H(\Sigma) = \frac{H^2}{2} + V_0(\Sigma) - \frac{(eH)^2}{2\pi^2}\Big\{\zeta'(-1,x) - \frac{1}{2}[x^2 - x]\ln x + \frac{x^2}{4}\Big\}, \tag{13}$$

where $x = \Sigma^2/(2eH)$, $\zeta(\nu, x)$ is the generalized Riemann zeta-function and $\zeta'(-1,x) = d\zeta(\nu,x)/d\nu|_{\nu=-1}$. The global minimum point of this function is the solution of the stationarity equation

$$\frac{\partial}{\partial\Sigma}V_H(\Sigma) = \frac{\Sigma}{4\pi^2}\{F(\Sigma) - I(\Sigma)\} = 0, \tag{14}$$

where $F(\Sigma)$ is given in (7), and

$$\begin{aligned} I(\Sigma) &= 2eH\Big\{\ln\Gamma(x) - \frac{1}{2}\ln(2\pi) + x - \frac{1}{2}(2x-1)\ln x\Big\} \\ &= \int_0^\infty \frac{ds}{s^2}\exp(-s\Sigma^2)[\ eHs\coth(eHs) - 1]. \end{aligned} \tag{15}$$

One can easily see that there exists, for arbitrary fixed values of H, G, only one non-trivial solution $\Sigma_0(H)$ of Eq. (14), which is the global minimum point of $V_H(\Sigma)$. There, $\Sigma_0(H)$ is a monotonically increasing function of H, and at $H \to \infty$

$$\Sigma_0(H) \approx \frac{eH}{\pi}\sqrt{\frac{G}{12}}. \tag{16}$$

However, at $H \to 0$

$$\Sigma_0^2(H) \approx \begin{cases} \frac{eH}{\pi}\exp\{-\frac{1}{eH}(\frac{4\pi^2}{G} - \Lambda^2)\}, & \text{if } G < G_c, \\ M^2, & \text{if } G > G_c. \end{cases} \tag{17}$$

So, at $G < G_c$ and $H = 0$ the NJL vacuum is chirally symmetric, but an arbitrarily small value of the external magnetic field H induces DCSB, and fermions acquire a non-zero mass $\Sigma_0(H)$ (the magnetic catalysis effect of DCSB).

Now let us consider the more general case, when $H \neq 0$ and $\mu \neq 0$. In one of our previous papers [29] an effective potential of a 3D Gross–Neveu model at non-zero H, μ and T was obtained. Similarly, one can find the effective potential in the NJL model I at $H, T, \mu \neq 0$:

$$V_{H\mu T}(\Sigma) = V_H(\Sigma) - \frac{TeH}{4\pi^2}\sum_{k=0}^{\infty}\alpha_k \int_{-\infty}^{\infty} dp \ln\left\{\left[1 + \exp^{-\beta(\varepsilon_k+\mu)}\right]\left[1 + \exp^{-\beta(\varepsilon_k-\mu)}\right]\right\}, \tag{18}$$

where $\beta = 1/T$, $\alpha_k = 2 - \delta_{0k}$, $\varepsilon_k = \sqrt{\Sigma^2 + p^2 + 2eHk}$, with $k = 0, 1, 2, ...$ denoting Landau levels, and the function $V_H(\Sigma)$ is given in (13). If we let the temperature in (18) tend to zero, we obtain the effective potential of the NJL model I at $H, \mu \neq 0$:

$$V_{H\mu}(\Sigma) = V_H(\Sigma) - \frac{eH}{4\pi^2}\sum_{k=0}^{\infty}\alpha_k \int_{-\infty}^{\infty} dp(\mu - \varepsilon_k)\theta(\mu - \varepsilon_k), \tag{19}$$

which, by performing the integration, can easily be cast into the form

$$V_{H\mu}(\Sigma) = V_H(\Sigma) - \frac{eH}{4\pi^2}\sum_{k=0}^{\infty}\alpha_k\theta(\mu - s_k)\left\{\mu\sqrt{\mu^2 - s_k^2} - s_k^2 \ln\left[\frac{\mu + \sqrt{\mu^2 - s_k^2}}{s_k}\right]\right\}, \tag{20}$$

where $s_k = \sqrt{\Sigma^2 + 2eHk}$. Finally, let us present the stationarity equation for the potential (20):

$$\frac{\partial}{\partial\Sigma}V_{H\mu}(\Sigma) \equiv \frac{\Sigma}{4\pi^2}\phi(\Sigma) = \frac{\Sigma}{4\pi^2}\left\{F(\Sigma) - I(\Sigma) + 2eH\sum_{k=0}^{\infty}\alpha_k\theta(\mu - s_k)\ln\left[\frac{\mu + \sqrt{\mu^2 - s_k^2}}{s_k}\right]\right\} = 0. \tag{21}$$

In order to get a phase portrait of the model under consideration we should find a one-to-one correspondence between points of the (μ, H)-plane and the global minimum points of the function (20), i.e. by solving Eq. (21) we should find the global minimum $\Sigma(\mu, H)$ of the potential (20) and then study its properties as a function of (μ, H).

3.1 The case $G < G_c$. Magnetic catalysis and chemical potential

In order to greatly simplify this problem, let us divide the (μ, H)-plane into a set of regions ω_k:

$$(\mu, H) = \bigcup_{k=0}^{\infty} \omega_k, \qquad \omega_k = \{(\mu, H) : 2eHk \leq \mu^2 \leq 2eH(k+1)\}. \tag{22}$$

In the ω_0 region only the first term from the series in (20) and (21) is non-vanishing. So, one can find that, for the points $(\mu, H) \in \omega_0$, which are above the line l=$\{(\mu, H) : \mu = \Sigma_0(H)\}$, the global minimum is at the point $\Sigma = 0$. Just under the curve l the point $\Sigma = \Sigma_0(H)$ is a local minimum of the potential (20), whereas $\Sigma = \Sigma_0(H)$ becomes a global minimum, when (μ, H) lies under the curve $\mu = \mu_c(H)$, which is defined by the following equation:

$$V_{H\mu}(0) = V_{H\mu}(\Sigma_0(H)). \tag{23}$$

Evidently, the line $\mu = \mu_c(H)$ is the critical curve of first-order phase transitions. In the ω_0 region Eq. (23) is easily solved:

$$\mu_c(H) = \frac{2\pi}{\sqrt{eH}}[V_H(0) - V_H(\Sigma_0(H))]^{1/2}. \tag{24}$$

Using the asymptotics (17) of the solution $\Sigma_0(H)$ at $H \to 0$, we find the following behaviour of $\mu_c(H)$ at $H \to 0$:

$$\mu_c(H) \approx \sqrt{\frac{eH}{2\pi}} \exp\Big\{-\frac{1}{2eH}\left(\frac{4\pi^2}{G} - \Lambda^2\right)\Big\}.$$

Hence, we have shown that at $\mu > \mu_c(H)$ ($G < G_c$) there exists a massless symmetric phase of the NJL model (numerical investigations of (20) and (21) give us a zero global minimum point for the potential $V_{H\mu}(\Sigma)$ in other regions $\omega_1, \omega_2, ...$ as well). The external magnetic field ceases to induce the DCSB at $\mu > \mu_c(H)$ (or at sufficiently small values of the magnetic field $H < H_c(\mu)$, where $H_c(\mu)$ is the inverse function of $\mu_c(H)$). However, under the critical curve (24) (or at $H > H_c(\mu)$), owing to the presence of an external magnetic field, the chiral symmetry is spontaneously broken. Here the magnetic field induces a dynamical fermion mass $\Sigma_0(H)$, which has a μ-independent value.

Lastly, we should also remark that in the NJL model (1) the magnetic catalysis effect takes place only in the phase with zero particle density, i.e. at $\mu < \mu_c(H)$. If $\mu > \mu_c(H)$, we have the symmetric phase with non-zero particle density, but here the magnetic field cannot induce DCSB.

3.2 The case $G < G_c$. Infinite cascade of massless phases

In the previous subsection we have shown that the points (μ, H), lying above the critical curve $\mu = \mu_c(H)$, correspond to the chirally symmetric ground state of the NJL model. Fermionic excitations of this vacuum have zero masses. At first sight, it might seem that the properties of this symmetric vacuum are slightly varied, when parameters μ and H are changed. However, this is not the case, and in the region $\mu > \mu_c(H)$ we have infinitely many massless symmetric

phases of the theory corresponding to infinitely many Landau levels, as well as a variety of critical curves of second-order phase transitions. Let us next prove this.

It is well known that the state of thermodynamic equilibrium (the ground state) of an arbitrary quantum system is described by the thermodynamic potential (TDP) Ω, which is just the value of the effective potential at its global minimum point. In the case under consideration, the TDP $\Omega(\mu, H)$ at $\mu > \mu_c(H)$ has the form

$$\begin{aligned}\Omega(\mu,H) &\equiv V_{H\mu}(0) = V_H(0) - \\ &-\frac{eH}{4\pi^2}\sum_{k=0}^{\infty}\alpha_k\theta(\mu-\epsilon_k)\Big\{\mu\sqrt{\mu^2-\epsilon_k^2}-\epsilon_k^2\ln\Big[\Big(\sqrt{\mu^2-\epsilon_k^2}+\mu\Big)/\epsilon_k\Big]\Big\}, \qquad (25)\end{aligned}$$

where $\epsilon_k = \sqrt{2eHk}$. We shall use the following criterion of phase transitions: if at least one first (second) partial derivative of $\Omega(\mu, H)$ is a discontinuous function at some point, then this is a point of a first- (second-) order phase transition.

Using this criterion, let us show that boundaries of ω_k regions (22), i.e. lines $l_k = \{(\mu, H) : \mu = \sqrt{2eHk}\}$ $(k = 1, 2, ...)$, are critical lines of second-order phase transitions. In an arbitrary ω_k region the TDP (25) has the form:

$$\begin{aligned}\Omega(\mu,H)|_{\omega_k} &\equiv \Omega_k = V_H(0) - \\ &-\frac{eH}{4\pi^2}\sum_{i=0}^{k}\alpha_i\theta(\mu-\epsilon_i)\left\{\mu\sqrt{\mu^2-\epsilon_i^2}-\epsilon_i^2\ln\left[\frac{(\sqrt{\mu^2-\epsilon_i^2}+\mu)}{\epsilon_i}\right]\right\}. \qquad (26)\end{aligned}$$

From (26) one easily finds

$$\frac{\partial\Omega_k}{\partial\mu}\Big|_{(\mu,H)\to l_{k+}} - \frac{\partial\Omega_{k-1}}{\partial\mu}\Big|_{(\mu,H)\to l_{k-}} = 0, \qquad (27)$$

as well as:

$$\frac{\partial^2\Omega_k}{(\partial\mu)^2}\Big|_{(\mu,H)\to l_{k+}} - \frac{\partial^2\Omega_{k-1}}{(\partial\mu)^2}\Big|_{(\mu,H)\to l_{k-}} = -\frac{eH\mu}{2\pi^2\sqrt{\mu^2-\epsilon_k^2}}\Big|_{\mu\to\epsilon_{k+}} \to -\infty. \qquad (28)$$

Equation (27) means that the first derivative $\partial\Omega/\partial\mu$ is a continuous function on all lines l_k. However, the second derivative $\partial^2\Omega/(\partial\mu)^2$ has an infinite jump on each line l_k (see (28)), so these lines are critical curves of second-order phase transitions. (Similarly, we can prove the discontinuity of $\partial^2\Omega/(\partial H)^2$ and $\partial^2\Omega/\partial\mu\partial H$ on all lines l_n.)

The results of the above investigations are presented in Fig. 3, where the phase portrait of the NJL model I at $G < G_c$ in the (μ, H)-plane is displayed.

3.3 The case $G > G_c$

Concerning supercritical values of the coupling constant, we shall consider here only the case $G_c < G < (1.225...)G_c$, where the phase portrait of the model I is qualitatively represented in Fig. 4. In this figure one can see infinite sets of symmetric massless $A_0, A_1, ...$ phases, as well as massive phases $C_0, C_1, ...$ with DCSB. In addition, there is another massive phase B.

Dashed and solid lines in Fig. 4 are critical curves of first- and second-order phase transitions, respectively. One can also see on this portrait infinitely many tricritical points t_k, s_k ($k = 0, 1, 2, ...$). For a fixed value of k the point t_k lies inside, but the point s_k is on the left boundary of the corresponding ω_k region (22). Each critical line l_k coincides with a part of the ω_k boundary. In Table 1, we give the values of the external magnetic field corresponding to tricritical points t_0 and s_0.

The presence of an infinite cascade of massless A_k-phases in the case $G > G_c$ may be proved in a way similar to what was done in the previous subsection. However, now an infinite set of massive chirally non-symmetric phases is available thanks to the particular structure of the function $\phi(\Sigma)$ in (21). A detailed numerical investigation of this function shows that, for some values of (μ, H) inside the C_k region (see Fig. 4), $\phi(\Sigma)$ as a function of Σ qualitatively behaves like the curve, drawn in the Fig. 5. At these values of (μ, H) there is only one non-trivial solution $\Sigma_k(\mu, H)$ of the stationary equation (21), which is the global minimum point of the effective potential (20) and at the same time is the quark mass in the phase C_k of the theory. Remark that in each phase C_k the quark mass is a μ-dependent function. In contrast, in the phase B, the global minimum point is equal to $\Sigma_0(H)$ (see (16), (17)), which is a μ-independent quantity. Hence, the particle density $n \equiv -\partial\Omega/\partial\mu$ in the ground state of phase B is identically equal to zero, whereas in each phase C_k this quantity differs from zero. This conclusion follows from the definition of the thermodynamic potential Ω given in the previous subsection , as well as from the fact that Ω has no μ-dependence in the phase B.[4]

If μ increases, the curve of Fig. 5 moves up and to the right side of this figure. So, for some values of μ the function $\phi(\Sigma)$ in (21) will have three zeros (see Fig. 6): the one on the left-hand side in this figure, Σ_{k+1}, is a local minimum of the function $V_{H\mu}(\Sigma)$, the one at the right-hand side, Σ_k ($\Sigma_k > \Sigma_{k+1}$), a global minimum of that function. If the chemical potential persists to grow, then at some critical value of μ the global minimum jumps from $\Sigma_k(\mu, H)$ to $\Sigma_{k+1}(\mu, H)$. At this moment we have a first-order phase transition from the massive phase C_k to the massive C_{k+1} one. In Fig. 4 the point of this phase transition lies on the curve $\overbrace{Mt_{k+1}}$, which is the boundary between regions C_k and C_{k+1}. Hence, all lines $\overbrace{Mt_k}$ in Fig. 4 ($k = 0, 1, 2, ...$) are first-order phase-transition curves. Here we should also remark that all points of the line $\overbrace{t_0\mu_c(H)}$ in this figure are described by Eq. (23). Since the phase structure of the model I is so complicated, the dynamical quark mass $\Sigma(\mu, H)$, which is given by the global minimum of the potential $V_{H\mu}(\Sigma)$, also has a rather complicated μ, H-dependence. For illustration, in Fig. 7 the schematic behaviour of $\Sigma(\mu, H)$ versus μ is presented at some fixed value of the external magnetic field H.

From standard textbooks on statistical physics (see, e.g. [4]) we know that more than three curves of first-order phase transitions (1OPT) should not intersect at one point of a phase diagram; not more than three phases are thus allowed to coexist in nature. However, in Fig. 4 one can see that infinitely many curves of 1OPT cross at the one point M. Indeed, this visible contradiction with the above-mentioned statement is only fictitious, because at the point M we have a second-order phase transition [14]. Hence, M does not belong to any of the critical curves of 1OPT $\overbrace{Mt_k}$ and is therefore not a point of phase coexistence.

[4] Since for all points of region B we have $\mu < \Sigma_0(H)$, it follows from (20) that $\Omega = V_{H\mu}(\Sigma_0(H)) = V_H(\Sigma_0(H))$, i.e. Ω has indeed no μ-dependence.

4. Magnetic oscillations in the model I

Now we want to show that there arise, from the presence of infinite sets of massless A_k phases as well as of massive C_k ones, magnetic oscillations (the so-called van Alphen–de Haas-type effect) of some physical parameters in the model I gauged by an external magnetic field.

4.1 The case $G < G_c$

Let the chemical potential be fixed, i.e. $\mu = \text{const} > \mu_{\text{c}}(\text{H})$. Then on the plane (μ, H) (see Fig. 3) we have a line that crosses critical lines $l_1, l_2, ...$ at points $H_1, H_2, ...$ The particle density n and the magnetization m of any thermodynamic system are defined by the TDP in the following way: $n = -\partial\Omega/\partial\mu$, $m = -\partial\Omega/\partial H$. At $\mu = \text{const}$ these quantities are continuous functions of the external magnetic field only, i.e. $n \equiv n(H)$, $m \equiv m(H)$. We know that all the second derivatives of $\Omega(\mu, H)$ are discontinuous on every critical line l_n. The functions $n(H)$ and $m(H)$, being continuous in the interval $H \in (0, \infty)$, therefore have first derivatives that are discontinuous on an infinite set of points $H_1, ..., H_k, ...$ Such a behaviour manifests itself as a phenomenon usually called oscillations.

In condensed-matter physics [3, 4] it is a conventional rule to separate the expression for a physical quantity with oscillations into two parts: the first one is called monotonic and does not contain any oscillations, whereas the second part, which is of particular interest here, contains all the oscillations. Following this rule, we can write down, say, the TDP (25) of the NJL model I in the form

$$\Omega(\mu, H) = \Omega_{mon}(\mu, H) + \Omega_{osc}(\mu, H). \tag{29}$$

In order to present the oscillating part $\Omega_{osc}(\mu, H)$ as well as the monotonic one $\Omega_{mon}(\mu, H)$ in an analytical form, we shall use the technique elaborated in [6], where manifestly analytical expressions for these quantities were found in the case of a perfectly relativistic electron–positron gas. This technique can be used without any difficulties in our case, too. So, applying in (25) the Poisson summation formula [4]

$$\sum_{n=0}^{\infty} \alpha_n \Phi(n) = 2 \sum_{k=0}^{\infty} \alpha_k \int_0^{\infty} \Phi(x) \cos(2\pi k x) dx, \tag{30}$$

one can get for $\Omega_{mon}(\mu, H)$ and $\Omega_{osc}(\mu, H)$ the following expressions

$$\Omega_{mon} = V_H(0) - \frac{\mu^4}{12\pi^2} - \frac{(eH)^2}{4\pi^3} \int_0^{\nu} dy \sum_{k=1}^{\infty} \frac{1}{k} P(\pi k y), \tag{31}$$

$$\Omega_{osc} = \frac{\mu}{4\pi^{3/2}} \sum_{k=1}^{\infty} \left(\frac{eH}{\pi k}\right)^{3/2} [Q(\pi k \nu) \cos(\pi k \nu + \pi/4) + P(\pi k \nu) \cos(\pi k \nu - \pi/4)], \tag{32}$$

where $\nu = \mu^2/(eH)$. (To find (31) and (32) it is sufficient to let the electron mass pass to zero in formula (19) of [6].) Functions $P(x)$ and $Q(x)$ in (31) and (32) are connected with Fresnel integrals $C(x)$ and $S(x)$ [30]

$$C(x) \;=\; \frac{1}{2} + \sqrt{\frac{x}{2\pi}} [P(x) \sin x + Q(x) \cos x]$$

$$S(x) \;=\; \frac{1}{2} - \sqrt{\frac{x}{2\pi}}[P(x)\cos x - Q(x)\sin x].$$

They have, at $x \to \infty$, the following asymptotics [30]:

$$P(x) = x^{-1} - \frac{3}{4}x^{-3} + ..., \quad Q(x) = -\frac{1}{2}x^{-2} + \frac{15}{8}x^{-4} + ...$$

Formula (32) presents, in a manifestly analytical form, the oscillating part of the TDP (25) for the NJL model at $G < G_c$. In the case under consideration, since the TDP is proportional to the pressure of the system, one can conclude that the pressure in the NJL model oscillates when $H \to 0$, too. It follows from (32) that the frequency of oscillations over the parameter $(eH)^{-1}$ equals $\mu^2/2$. Then, starting from (32), one can easily find the corresponding expressions for the oscillating parts of $n(H)$ and $m(H)$. These quantities oscillate at $H \to 0$ with the same frequency $\mu^2/2$ and have a rather involved form, so we do not present them here.

Finally, we should note that the character of magnetic oscillations in the NJL model at $G < G_c$ resembles the magnetic oscillations in massless quantum electrodynamics [5, 6]. This circumstance is conditioned by the resemblance of the vacuum properties in the two models. Indeed, both in the NJL model and in QED, for fixed μ and varying values of H, there are infinitely many second-order phase transitions (see the appendix, where the vacuum structure of QED at $\mu, H \neq 0$ is considered).

4.2 The case $G_c < G < (1.225...)G_c$

Here at $\mu > \mu_{1c}(M)$ (see Fig. 4) the TDP of the NJL model as well as all thermodynamical parameters of the system oscillate with the frequency $\mu^2/2$. This can be shown in a way similar to what was done in the previous section.

However, at $M < \mu < \mu_{1c}(M)$, the character of magnetic oscillations is changed. Let us next prove this. First of all, in this case we have another expression for the TDP of the system

$$\Omega(\mu, H) = V_{H\mu}(\Sigma(\mu, H)), \tag{33}$$

where $V_{H\mu}(\Sigma)$ is given in (20) and $\Sigma(\mu, H)$ is the non-trivial solution of the stationarity equation (21). In each of the massive phases C_k the μ- and H-dependent function $\Sigma(\mu, H)$ coincides with the corresponding fermionic mass $\Sigma_k(\mu, H)$ (see subsection 3.3). Using in (20) again the Poisson summation formula (30), one can easily select the oscillating part of the TDP (33) in a manifestly analytical form

$$\begin{aligned}\Omega_{osc}(\mu, H) \;&=\; \frac{\mu\theta(\mu - \Sigma(\mu, H))}{4\pi^{3/2}} \sum_{k=1}^{\infty} \left(\frac{eH}{\pi k}\right)^{3/2} [Q(\pi k\nu)\cos(2\pi k\omega + \pi/4) + \\ &+ P(\pi k\nu)\cos(2\pi k\omega - \pi/4)],\end{aligned} \tag{34}$$

where $\nu = \mu^2/(eH)$, $\omega = (\mu^2 - \Sigma^2(\mu, H))/(2eH)$. From (34) one can see that as a function of the variable $(eH)^{-1}$, the TDP (33) oscillates with frequency $(\mu^2 - \Sigma^2(\mu, H))/2$ if this variable tends to infinity. Since $\Omega(\mu, H)$ is equal, up to a sign, to the pressure in the ground state of the system, also in the present case the pressure in the NJL model is an oscillating quantity.

Moreover, taking into account the stationarity equation (21), one can easily derive manifest expressions for oscillating parts of other thermodynamic quantities such as particle density $n = -\partial\Omega/\partial\mu$ and magnetization $m = -\partial\Omega/\partial H$ from (33) and (34),

$$\begin{aligned} m_{osc} &= -\frac{(\mu^2 - \Sigma^2(\mu,H))^{3/2}}{4\sqrt{2}\pi^3\mu\omega^{1/2}} \sum_{k=1}^{\infty} \frac{\sin(2\pi k\omega - \pi/4)}{k^{3/2}} + o\left(\frac{1}{\omega^{1/2}}\right), \\ n_{osc} &= \frac{(\mu^2 - \Sigma^2(\mu,H))^{3/2}}{4\sqrt{2}\pi^3\mu\omega^{3/2}} \sum_{k=1}^{\infty} \frac{\sin(2\pi k\omega - \pi/4)}{k^{3/2}}. \end{aligned} \tag{35}$$

It is clear from (35) that particle density and magnetization in the ground state of the NJL model oscillate with the same frequency as Ω.

Comparing magnetic oscillations in the NJL model I and in QED, we see three main differences. Let us remark that in QED the frequency of magnetic oscillations (over the variable $(eH)^{-1}$) is equal to $(\mu^2 - M^2)/2$, where M is the electron mass [6]. In the NJL model, in contrast to QED, the magnetic oscillation frequency is an H-dependent quantity. So, strictly speaking, in the NJL model magnetic oscillations are not periodic ones. Similar peculiarities of magnetic oscillations are observed in some ferromagnetic semiconductive materials such as $HgCr_2Se_4$ [31], where non-periodic magnetic oscillations over the variable $(eH)^{-1}$ were found to exist for electric conductivity[5] as well as magnetization. This is the first distinction.

A second difference is the character of the oscillations in the two models: in QED, magnetic oscillations are accompanied by second-order phase transitions (see Appendix), while in the NJL model they occur as a result of an infinite cascade of first-order phase transitions.

Thirdly, we should remark that in the NJL model not only thermodynamic quantities oscillate, but some dynamical parameters of the system do as well. This concerns, in particular, oscillations of the dynamical quark mass. In fact, by applying the Poisson summation formula (30) in the stationarity equation (21) and searching for the solution $\Sigma(\mu,H)$ of this equation in the form $\Sigma(\mu,H) = \Sigma_{mon} + \Sigma_{osc}$, one can easily find the following expressions for $H \to 0$:

$$\begin{aligned} \Sigma_{osc} &= \frac{(\mu^2 - \tilde{M}^2)^{3/2}}{\sqrt{2}\pi\mu\tilde{\omega}^{3/2} f'(\tilde{M})} \sum_{k=1}^{\infty} \frac{\sin(2\pi k\tilde{\omega} - \pi/4)}{k^{3/2}} + o\left(\frac{1}{\omega^{3/2}}\right), \\ \Sigma_{mon} &= \tilde{M} + \frac{\mu(\mu^2 - \tilde{M}^2)^{3/2}}{12\tilde{M}^2 f'(\tilde{M})\tilde{\omega}^2} \left[1 + \frac{\sqrt{\mu^2 - \tilde{M}^2}}{\mu}\right] + o\left(\frac{1}{\omega^{3/2}}\right), \end{aligned} \tag{36}$$

where $\tilde{\omega} = (\mu^2 - \tilde{M}^2)/2(eH)$, $\tilde{M} \equiv \Sigma_0(\mu)$ is the quark mass at $H = 0$, $\mu \neq 0$ (see Fig. 2) and

$$f(x) = F(x) + 2\mu\sqrt{\mu^2 - x^2} - 2x^2 \ln\frac{\mu + \sqrt{\mu^2 - x^2}}{x}$$

($F(\Sigma)$ is defined in (7)). Hence, in the framework of the NJL model I the quark mass $\Sigma(\mu,H)$, as well as other dynamical quantities composed from it, oscillate in the presence of an external magnetic field.

[5]Magnetic oscillations of the electric conductivity, which is proportional to the particle density, are known as the Shubnikov–de Haas effect [3].

5. Magnetic oscillations in the model II

Next, let us consider magnetic oscillations in the more realistic NJL model II containing two kinds of quarks: u- and d-quarks with electric charges e_1 and e_2, respectively. The effective potential $v_{h\mu}$ in the case under consideration is a trivial generalization of $V_{H\mu}$ derived in the one-flavour case

$$v_{h\mu}(\Sigma) = -\frac{H^2}{2} - \frac{\Sigma^2}{2G} + \sum_{i=1}^{2} V_{e_i H\mu}(\Sigma), \tag{37}$$

where $\Sigma = \sqrt{\sigma^2 + \vec{\pi}^2}$, and $V_{e_i H\mu}(\Sigma)$ is equal to $V_{H\mu}(\Sigma)$ (20), with e replaced by $|e_i|$.

Qualitatively, the phase structure of the NJL model II is the same as that of model I. So, at $G < G_c$ we have an infinite set of massless phases (similar to the phase portrait of the model I in Fig. 3) reflecting the infinite set of Landau levels that is the basis for magnetic oscillations. Using the analytical methods of section 4, one can easily select in the present case the oscillating part of the thermodynamic potential:

$$\Omega_{osc} = \frac{\mu}{4\pi^{3/2}} \sum_{i=1}^{2} \sum_{k=1}^{\infty} \left(\frac{|e_i|H}{\pi k}\right)^{3/2} [Q(\pi k \nu_i)\cos(\pi k \nu_i + \pi/4) + P(\pi k \nu_i)\cos(\pi k \nu_i - \pi/4)], \tag{38}$$

where $\nu_i = \mu^2/(|e_i|H)$. Hence, in the model II, in contrast to the model I and QED, we have a superposition of two oscillating modes. At growing values of the parameter $(eH)^{-1}$, the frequency of oscillations in each of the modes is equal to $e\mu^2/(2|e_i|)$.

At $G_c < G$ there is a finite vicinity of G_c in which the phase portrait of the model II in the (μ, H)-plane is similar to the one in the model I (see Fig. 4). So, in the case under consideration we have infinite sets of massless and massive phases as well. The cascade of massive phases is the foundation for non-periodic magnetic oscillations. Indeed, from (37) it follows that the oscillating part of TDP has the form

$$\begin{aligned} \Omega_{osc}(\mu, H) \;=\; & \frac{\mu\theta(\mu - \Sigma(\mu,H))}{4\pi^{3/2}} \sum_{i=1}^{2} \sum_{k=1}^{\infty} \left(\frac{|e_i|H}{\pi k}\right)^{3/2} [Q(\pi k \nu_i)\cos(2\pi k \omega_i + \pi/4) + \\ & + P(\pi k \nu_i)\cos(2\pi k \omega_i - \pi/4)], \end{aligned} \tag{39}$$

where $\nu_i = \mu^2/(|e_i|H)$, $\omega_i = (\mu^2 - \Sigma^2(\mu,H))/(2|e_i|H)$, and $\Sigma(\mu, H)$ is the global minimum point of the effective potential (37). As in the previous model, $\Sigma(\mu, H)$ in the present case is an H-dependent function. This means that magnetic oscillations in the NJL model II are composed of two non-periodic harmonics, because each of them has, as a function of the variable $(eH)^{-1}$, the H-dependent frequency $e(\mu^2 - \Sigma^2(\mu,H))/(2|e_i|)$.

6. Summary and conclusions

In the present paper we have studied the magnetic properties of a many-body system of cold and dense quark matter with four-fermion interactions. In particular, we have investigated the ground-state (vacuum) structure of two simple NJL models with one or two quark flavours, respectively, which are taken at non-zero chemical potential μ and magnetic field H.

As it turns out, in both types of models there exists a phase B (see Figs. 3 and 4) in which the quark mass is equal to $\Sigma_0(H)$, i.e. it is a μ-independent quantity. Since this phase is achieved in the region $\mu < \Sigma_0(H)$, the resulting particle density is expected to be zero, which is supported by our calculation. Clearly, this is in agreement with the physical interpretation of the chemical potential as the energy required to create one particle in the system. Indeed, the energy μ, which in the phase B is smaller than the quark mass, is not sufficient to create a particle, so that in the ground state of this phase the particle density must vanish.

Most interestingly, we have shown that in NJL models there exist an infinite set of massless chirally invariant phases (phases $A_0, A_1, ...$ in Figs. 3 and 4), which lead to periodic magnetic oscillations of some thermodynamic quantities of the system (so-called van Alphen–de Haas effect). In NJL models, this effect is observed at weak couplings ($G < G_c$, where $G_c = 4\pi^2/\Lambda^2$) or at sufficiently high values of the chemical potential and resembles magnetic oscillations in massless QED.

Furthermore, for some finite interval of the coupling constant $G_c < G < G_1$, where in the framework of the model I $G_1 = (1.225...)G_c$, the phase structure of NJL models I and II contains an infinite set of massive chirally non-invariant phases (phases $C_0, C_1, ...$ in Fig. 4). This is the basis for non-periodic magnetic oscillations of some thermodynamic parameters, since the dynamical quark mass in each of the phases C_k is now itself an H-dependent quantity. (Notice that analogous non-periodic magnetic oscillations were recently found to exist in some condensed-matter materials [31], too.) We should also remark that, at $G_c < G < G_1$, some dynamical parameters in NJL systems, such as quark masses, oscillate over $(eH)^{-1}$ as well. This is an unknown fact in the standard condensed-matter theory of the van Alphen–de Haas effect.

Moreover, our numerical analysis shows that for values of the coupling constant $G \in (G_1, G_2)$, where $G_2 \approx 40G_c$, we have in both models a finite number of massive phases C_k (the number of massless phases is infinite as before). At larger values of the coupling constant, i.e. at $G > G_2$, there exist no massive phases in the phase structure of NJL models at all, except the trivial phase B.

Finally, it is interesting to note that for fixed magnetic field H the dynamical quark mass $\Sigma(\mu, H)$ of NJL models discontinuously jumps as a function of μ, at points $\mu_0, \mu_1, \mu_2, ...$ (see Fig. 7), thus reflecting the structure of the underlying phase portrait shown in Fig. 4.

In conclusion, we have shown that NJL models at $\mu, H \neq 0$ exhibit an interesting phase structure and a set of oscillating quantities, which are richer than in the corresponding QED case. Note also that the above approach can be further employed for a combined study of quark and diquark condensates of NJL models taken at $\mu, H \neq 0$. Work in this direction is under way.

One of the authors (D.E.) gratefully acknowledges the kind support and warm hospitality of the colleagues of the Theory Division at CERN. This work was supported in part by the Russian Fund for Fundamental Research, project 98-02-16690, and by DFG-project 436 RUS 113/477.

Appendix

The QED vacuum structure in the presence of μ and H.

In the framework of QED and in a one-loop approximation, the effective Lagrangian in the presence of an external homogeneous magnetic field has the following form [5, 6]:

$$L_{eff}(\mu, H) = L_1(H) - \Omega_{QED}(\mu, H), \qquad (A.1)$$

where $L_1(H)$ is the Lagrangian at $\mu = 0, H \neq 0$. Since it does not influence the phase structure of QED, we do not present its explicit form here, but refer to [5, 6]. The second part of $L_{eff}(\mu, H)$ is exactly the thermodynamic potential of a perfect electron–positron gas

$$\Omega_{QED}(\mu, H) = -\frac{eH}{4\pi^2}\sum_{n=0}^{\infty}\alpha_n\theta(\mu-\epsilon_n)\Big\{\mu\sqrt{\mu^2-\epsilon_n^2} - \epsilon_n^2\ln\Big[(\sqrt{\mu^2-\epsilon_n^2}+\mu)/\epsilon_n\Big]\Big\}. \qquad (A.2)$$

In (A.2) we have introduced the notation: $\epsilon_n = \sqrt{M^2+2eHn}$, where M is the electron mass at $H = 0, \mu = 0$, and $\alpha_n = 2 - \delta_{0n}$.

Using the results and methods of subsection 3.2 one can now easily show that, on each line $l_n = \{(\mu, H) : \mu = \sqrt{M^2+2eHn}\}$ of the (μ, H)-plane, all second derivatives of $L_{eff}(\mu, H)$ (A.1) are discontinuous. So, the lines l_n $(n = 0, 1, ...)$ in Fig. 8 are the curves of second-order phase transitions. They divide the (μ, H)-plane into an infinite set of regions C_n $(n = 0, 1, ...)$ corresponding to different massive phases of QED (associated to Landau levels) with the same electron mass M. Nevertheless, each phase C_n is characterized by such physical quantities as particle density $n(\mu, H)$ and magnetization $m(\mu, H)$. On each phase boundary l_n these quantities are continuous functions. However, their first derivatives are discontinuous functions on each line l_n, so the derivative jump of n or m is the signal of a second-order phase transition.

As in the previously considered case (see subsection 3.3 and Fig. 4) the point M in Fig. 8, where all lines l_n intersect, is a special point differing from other points of the lines l_n. Indeed, at $H = 0$ we have [6]

$$\Omega_{QED}(\mu, 0) = -\frac{\theta(\mu-M)}{6\pi^2}\int_M^{\mu}\frac{xdx}{\sqrt{x^2-M^2}}(\mu-x)^2(\mu+2x). \qquad (A.3)$$

It follows from (A.3) that only the third derivative $\partial^3\Omega_{QED}(\mu, 0)/(\partial\mu)^3$ is a discontinuous function at the point $\mu = M$. At the same time, in other points of critical curves l_n, already the second derivative $\partial^2\Omega_{QED}(\mu, H)/(\partial\mu)^2$ is discontinuous.

Here we have considered only the relativistic case, but one can easily show that the non-relativistic electron gas at $\mu, H \neq 0$ has an infinite cascade of massive phases, too. So, at the basis of the van Alphen–de Haas and Shubnikov–de Haas effects lies an infinite set of second-order phase transitions.

References

[1] D. Bailin and A. Love, Phys. Rep. **107**, 325 (1984); R. Rapp, T. Schafer, E.V. Shuryak and M. Velkovsky, Phys. Rev. Lett. **81**, 53 (1998); M. Alford, K. Rajagopal and F. Wilczek, Phys. Lett. **B422**, 247 (1998).

[2] S. Schramm, B. Muller and A.J. Schramm, Mod. Phys. Lett. **A7**, 973 (1992); I.A. Shushpanov and A.V. Smilga, Phys. Lett. **B 402**, 351 (1997); J. Rafelsky, *Electromagnetic Fields in the QCD-Vacuum*, hep-ph/9806389.

[3] W.J. de Haas and P.M. van Alphen, Proc. Amsterdam Acad. **33**, 1106 (1936); D. Shoenberg, *Magnetic Oscillations in Metals*, (Cambridge University Press, Cambridge, 1984); I.M. Lifshitz, *Selected Works. Electronic Theory of Metals, Physics of Polymers and Bipolymers* [in Russian], (Nauka, Moscow, 1994).

[4] E.M. Lifshitz and L.P. Pitaevski, *Statistical Physics*, (Pergamon, Oxford, 1980); Yu.B. Rumer and M.Sh. Ryvkin, *Thermodynamics, Statistical Physics and Kinetics* [in Russian], (Nauka, Moscow, 1977).

[5] P. Elmfors, D. Persson and B.-S. Skagerstam, Phys. Rev. Lett. **71**, 480 (1993); Astropart. Phys. **2**, 299 (1994); D. Persson and V. Zeitlin, Phys. Rev. **D 51**, 2026 (1995); J.O. Andersen and T. Haugset, Phys. Rev. **D 51**, 3073 (1995); V.Ch. Zhukovsky, T.L. Shoniya and P.A. Eminov, J. Exp. Theor. Phys. **80**, 158 (1995); V.Ch. Zhukovsky, A.S. Vshivtsev and P.A. Eminov, Phys. Atom. Nucl. **58**, 1195 (1995); V.R. Khalilov, Phys. Atom. Nucl. **61**, 1520 (1998).

[6] A.S. Vshivtsev and K.G. Klimenko, J. Exp. Theor. Phys. **82**, 514 (1996).

[7] S. Chakrabarty, Phys. Rev. **D 54**, 1306 (1996).

[8] Y. Nambu and G. Jona-Lasinio, Phys. Rev. **122**, 345 (1961); **124**, 246 (1961).

[9] V.G. Vaks and A.I. Larkin, Sov. Phys. JETP **13**, 192 and 979 (1961); B.A. Arbuzov, A.N. Tavkhelidze and R.N. Faustov, Sov. Phys. Dokl. **6**, 598 (1962).

[10] D. Ebert and M. K. Volkov, Yad. Fiz. **26**, 1265 (1982); Z. Phys. **C 16**, 205 (1983); D. Ebert and H. Reinhardt, Nucl. Phys. **B 271**, 188 (1986).

[11] M.K. Volkov, Ann. Phys. **157**, 282 (1984); D. Ebert, H. Reinhardt and M.K. Volkov, Progr. Part. Nucl. Phys. **33**, 1 (1994).

[12] S.P. Klevansky, Rev. Mod. Phys. **64**, 649 (1992).

[13] S. Kawati and H. Miyata, Phys. Rev. **D 23**, 3010 (1981); J. Fuchs, Z. Phys. **C 22**, 83 (1984); V. Bernard, U.-G. Meissner and I. Zahed, Phys. Rev. **D 36**, 819 (1987); Chr.V. Christov and K. Goeke, Acta Phys. Pol. **B 22**, 187 (1991); D. Ebert, Yu.L. Kalinovsky, L. Münchow and M.K. Volkov, Int. J. Mod. Phys. **A 8**, 1295 (1993).

[14] A.S. Vshivtsev and K.G. Klimenko, JETP Lett. **64**, 338 (1996); hep-ph/9701288;
A.S. Vshivtsev, V.Ch. Zhukovsky and K.G. Klimenko, J. Exp. Theor. Phys. **84**, 1047 (1997).

[15] S.P. Klevansky and R.H. Lemmer, Phys. Rev. **D 39**, 3478 (1989).

[16] D. Ebert and M.K. Volkov, Phys. Lett. **B 272**, 86 (1991);
I.A. Shovkovy and V.M. Turkowski, Phys. Lett. **B 367**, 213 (1995);
D. Ebert and V.Ch. Zhukovsky, Mod. Phys. Lett. **A 12**, 2567 (1997).

[17] V.P. Gusynin, V.A. Miransky and I.A. Shovkovy, Phys. Lett. **B 349**, 477 (1995).

[18] T. Inagaki, T. Muta and S.D. Odintsov, Mod. Phys. Lett. **A 8**, 2117 (1993);
E. Elizalde, S. Leseduarte and S.D. Odintsov, Phys. Rev. **D 49**, 5551 (1994);
H. Forkel, Phys. Lett. **B 280**, 5 (1992); Nucl. Phys. **A 581**, 557 (1995);
D.K. Kim and I.G. Koh, Phys. Rev. **D 51**, 4573 (1995);
E.J. Ferrer, V.P. Gusynin and V. de la Incera, hep-ph/9901446.

[19] A.S. Vshivtsev, A.K. Klimenko and K.G. Klimenko, Phys. Atom. Nucl. **61**, 479 (1998);
M.A. Vdovichenko, A.S. Vshivtsev and K.G. Klimenko, preprint IFVE 97-59, Protvino, 1997 [in Russian]; A.S. Vshivtsev, M.A. Vdovichenko and K.G. Klimenko, J. Exp. Theor. Phys. **87**, 229 (1998).

[20] T. Inagaki, T. Muta and S.D. Odintsov, Progr. Theor. Phys. Suppl. **127**, 93 (1997).

[21] D.M. Gitman, S.D. Odintsov and Yu.I. Shil'nov, Phys. Rev. **D 54**, 2964 (1996);
B. Geyer, L.N. Granda and S.D. Odintsov, Mod. Phys. Lett. **A 11**, 2053 (1996).

[22] L. Dolan and R. Jackiw, Phys. Rev. **D 9**, 3320 (1974).

[23] K.G. Klimenko, Theor. Math. Phys. **89**, 1161 (1992); K.G. Klimenko, Z. Phys. **C 54**, 323 (1992); K.G. Klimenko, A.S. Vshivtsev and B.V. Magnitsky, Nuovo Cim. **A 107**, 439 (1994).

[24] V.P. Gusynin, V.A. Miransky and I.A. Shovkovy, Phys. Rev. Lett. **73**, 3499 (1994).

[25] K.G. Klimenko, preprint IHEP 98-56, Protvino, 1998; hep-ph/9809218.

[26] J. Schwinger, Phys. Rev. **82**, 664 (1951).

[27] M.R. Brown and M.J. Duff, Phys. Rev. **D 11**, 2124 (1975);
W. Dittrich, Fortschr. Phys. **26**, 289 (1978).

[28] A.P. Prudnikov, Yu.A. Brychkov and O.I. Marichev, *Integrals and Series,* (Gordon and Breach, New York, 1986).

[29] A.S. Vshivtsev, K.G. Klimenko and B.V. Magnitsky, Theor. Math. Phys. **106**, 319 (1996).

[30] H. Bateman and A. Erdeyi, *Higher Transcendental Functions,* (McGrawHill, New York, 1953).

[31] A.D. Balaev et al., Zh. Eksp. Teor. Fiz. **113**, 1877 (1998) [in Russian].

Figure captions

Fig. 1 Phase portrait of the NJL model at non-zero μ and for arbitrary values of the fermion mass M. Phases B and C are massive and non-symmetric, A is a chirally symmetric phase. Here $\mu_{2c}(M) = M$, $\mu_{1c}(M) = \sqrt{\frac{1}{2}M^2 \ln(1+\Lambda^2/M^2)}$, $\mu_{3c}(M)$ is the solution of the equation $V_\mu(0) = V_\mu(M)$, $M_{2c} = \Lambda/(2.21...)$, M_{1c} is the solution of the equation $\mu_{1c}^2(M_{1c}) = \Lambda^2/(4e)$. In phase B the particle density in the ground state is equal to zero, whereas in phase C it is non zero. Solid and dashed lines represent critical curves of second- and first-order phase transitions, respectively; α and β denote tricritical points.

Fig. 2 The behaviour of the dynamical quark mass $\Sigma_0(\mu)$ as a function of μ for the case $M < M_{1c}$ and $H = 0$ within the framework of the model I.

Fig. 3 Phase portrait of the gauged model I at $G < G_c$. Solid lines l_k are given by $l_k = \{(\mu, H) : \mu = \sqrt{2eHk}\}$. They are critical curves of second-order phase transitions. The dashed line of first-order phase transitions is defined by Eq. (23).

Fig. 4 Phase portrait of the gauged model I at $G_c < G < (1.225...)G_c$. Here M is the quark mass at $\mu = 0, H = 0$, and the quantity $\mu_{1c}(M)$ is presented in Fig. 1. The dashed line $\overbrace{t_0\mu_c(H)}$ is defined by Eq. (23). In this case one has infinite sets of symmetric massless phases $A_0, A_1, ...$ as well as massive phases $C_0, C_1, ...$ with DCSB. In addition there exists another massive phase B.

Fig. 5 Typical behaviour of $\phi(\Sigma)$ (21) for some points $(\mu, H) \in C_k$. Here $\sigma_n = \sqrt{\mu^2 - 2eHn}$.

Fig. 6 For increasing μ, there arise three zeroes of the function $\phi(\Sigma)$ (21) defining two local minima Σ_k and $\Sigma_{k+1}(\Sigma_{k+1} < \Sigma_k)$ of the effective potential, respectively. The global minimum of $V_{H\mu}(\Sigma)$ lies in one of them and passes by a jump from one local minimum to another one depending on the values of μ.

Fig. 7 Schematic representation of the dynamical quark mass $\Sigma(\mu, H)$ as function of μ for fixed magnetic field qualitatively reflecting the structure of the phase portrait in Fig. 4. Here the magnetic field is fixed in the interval (H_{s_2}, H_{t_2}), where s_2, t_2 are tricritical points (see Fig. 4). The μ_k,$\tilde{\mu}_c(H)$ $(k = 0, 1, 2)$ are the values of the chemical potential at which the line $H =$ const crosses in Fig. 4 the critical curves $\overbrace{Mt_k}$ and $\overbrace{s_2t_2}$, respectively.

Fig. 8 Phase portrait of QED at $\mu, H \neq 0$. All the lines l_n are the curves of second-order phase transitions.

Table caption

Table 1. Values of the external magnetic field corresponding to tricritical points t_0 and s_0 (see Fig. 4) for different ratios of coupling constants G/G_c.

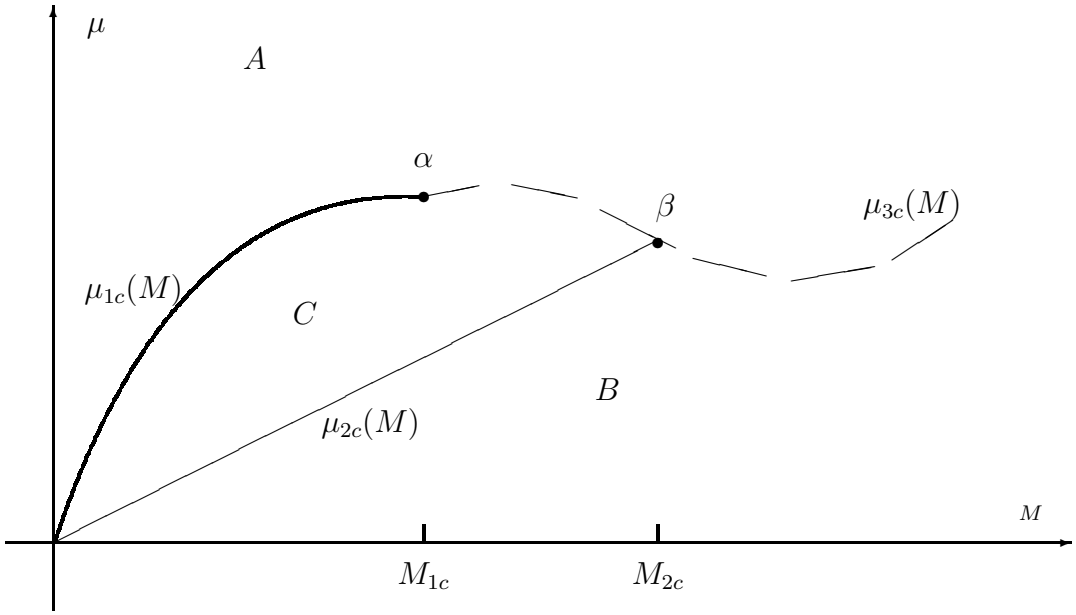

Fig. 1

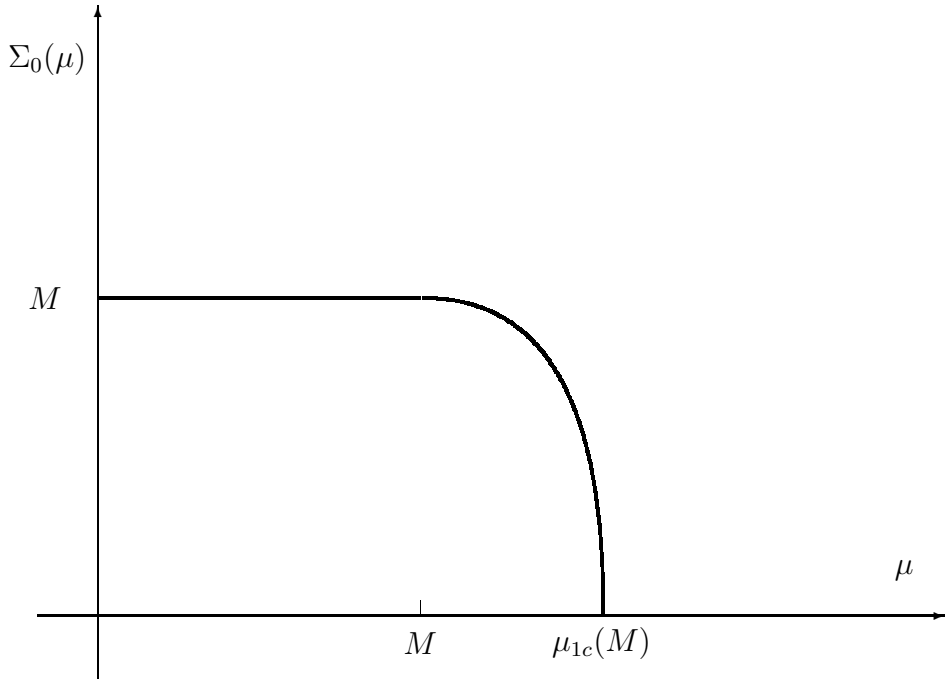

Fig. 2

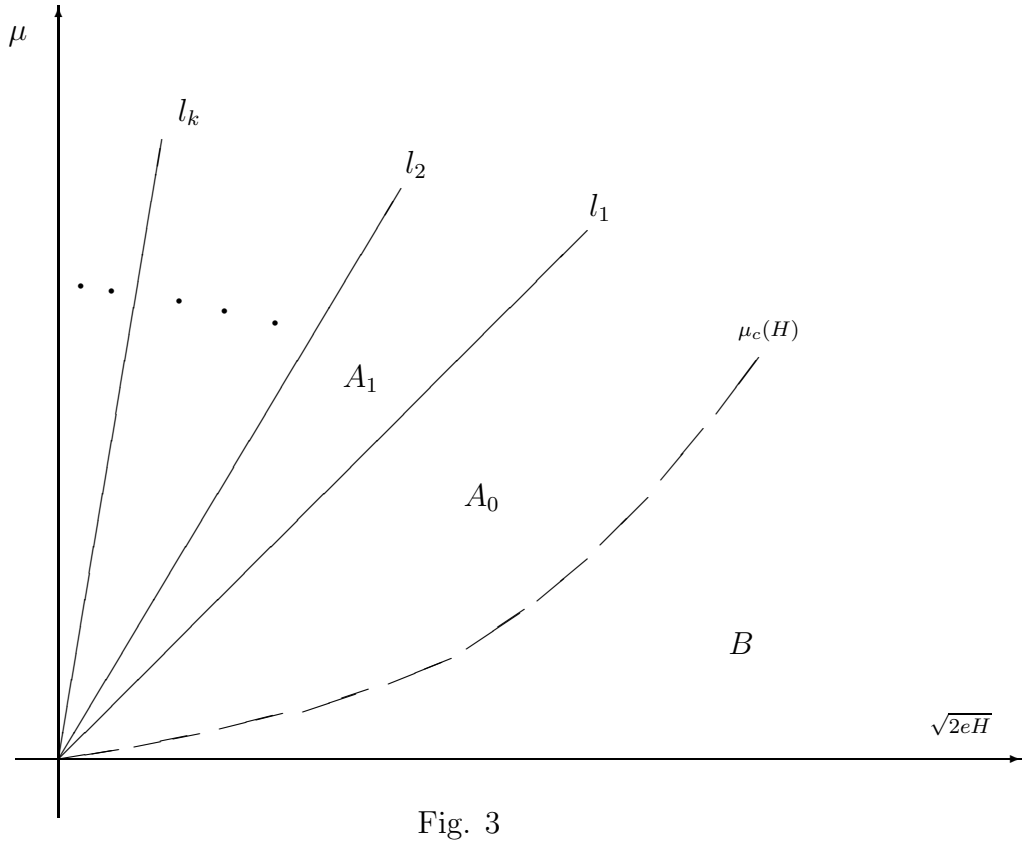

Fig. 3

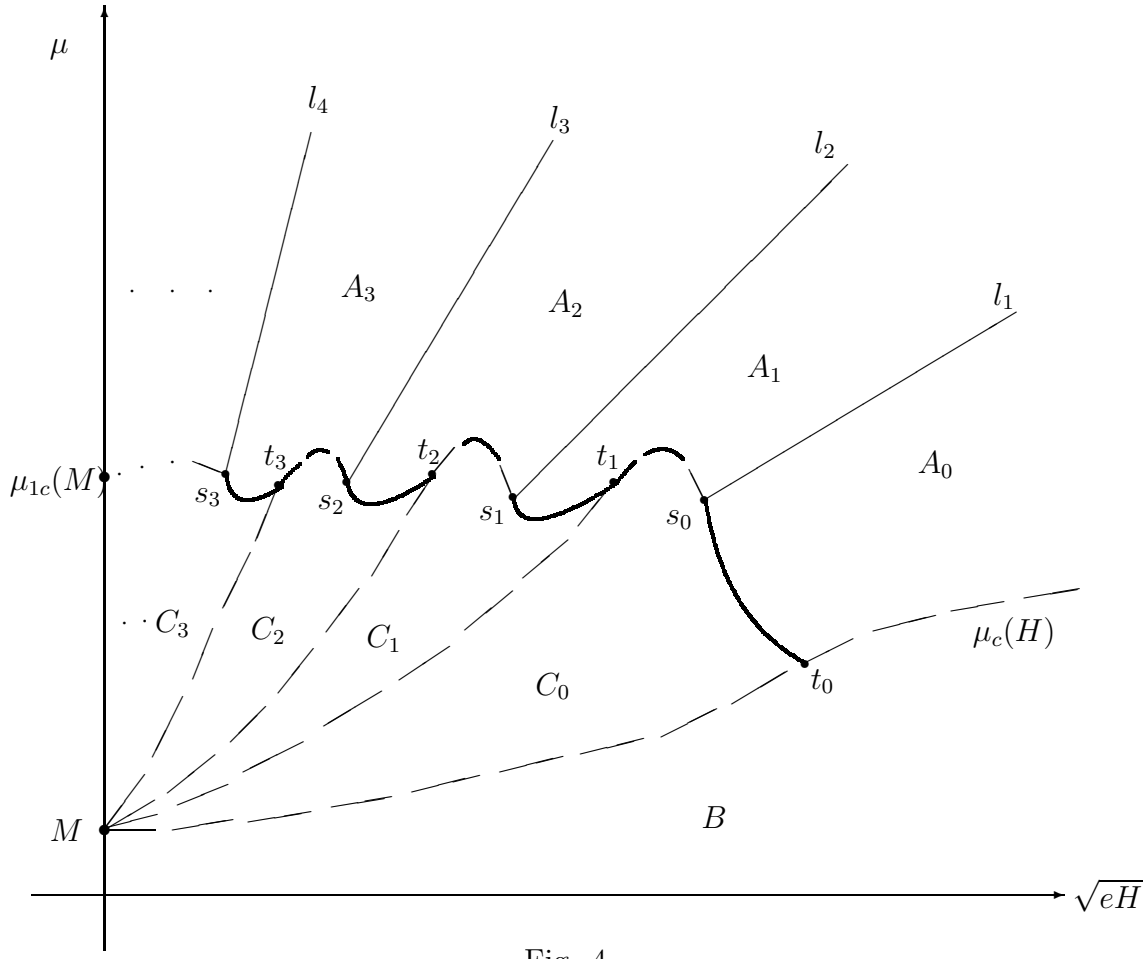
μ
l_4
l_3
l_2
l_1
A_3
A_2
A_1
A_0
$\mu_{1c}(M)$
t_3
t_2
t_1
s_3
s_2
s_1
s_0
C_3
C_2
C_1
C_0
$\mu_c(H)$
t_0
M
B
$\sqrt{eH}$

Fig. 4

G/G_c	1.01	1.1	1.15	1.2
eH_{t_0}/Λ^2	0.0129...	0.08119...	0.10769...	0.12987...
eH_{s_0}/Λ^2	0.00614...	0.05639...	0.08088...	0.10338...

Table 1

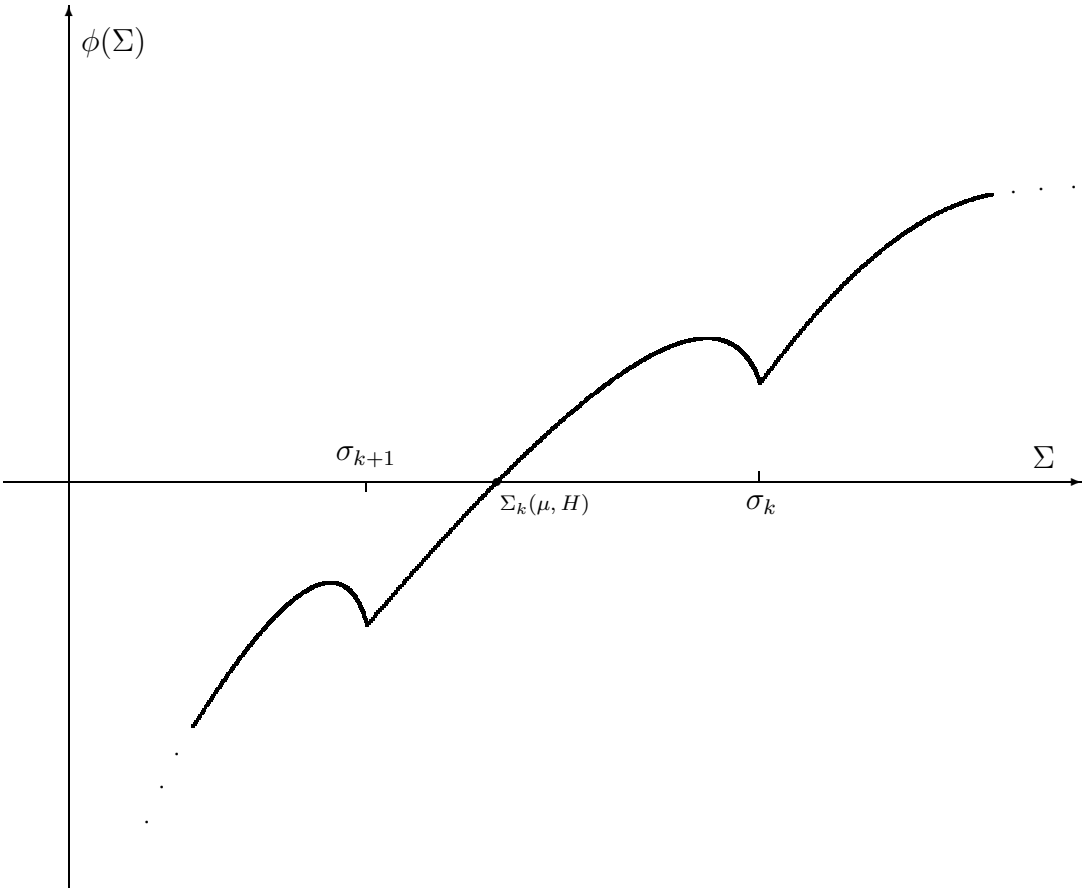

Fig. 5

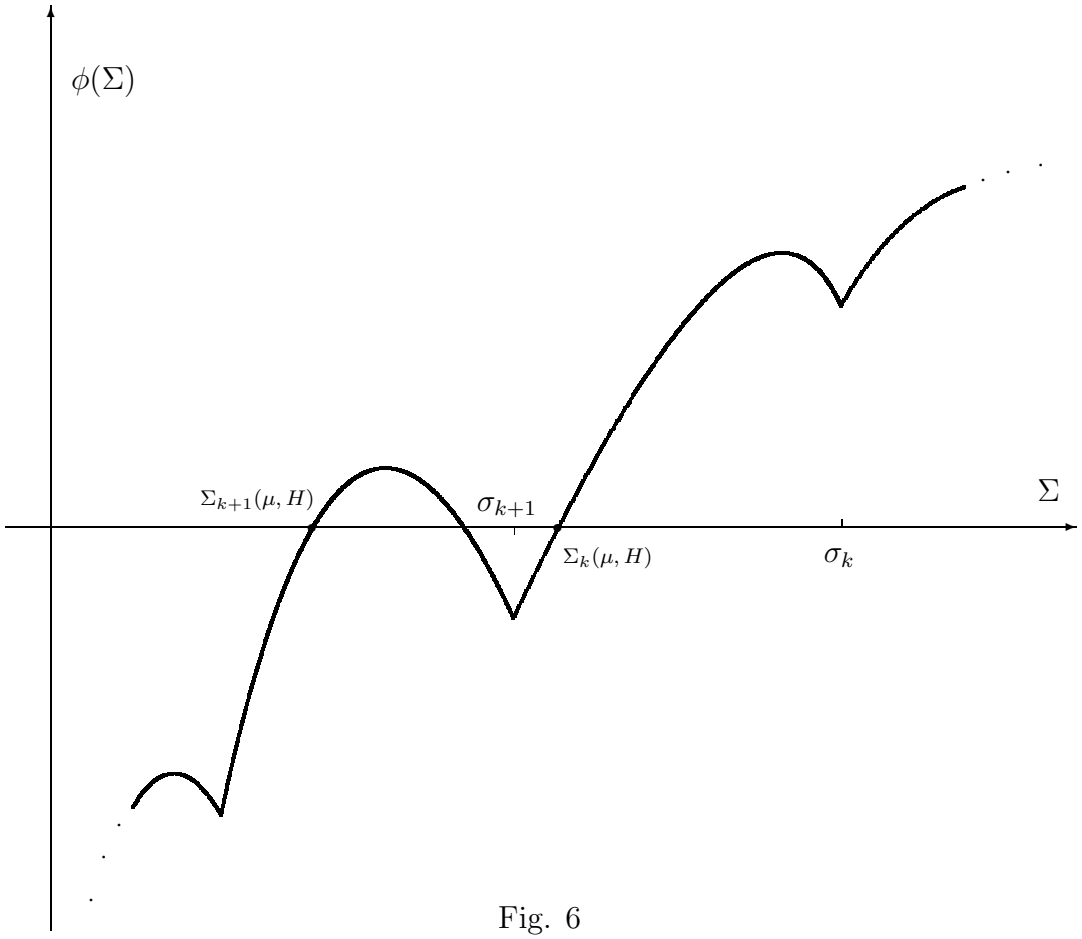

Fig. 6

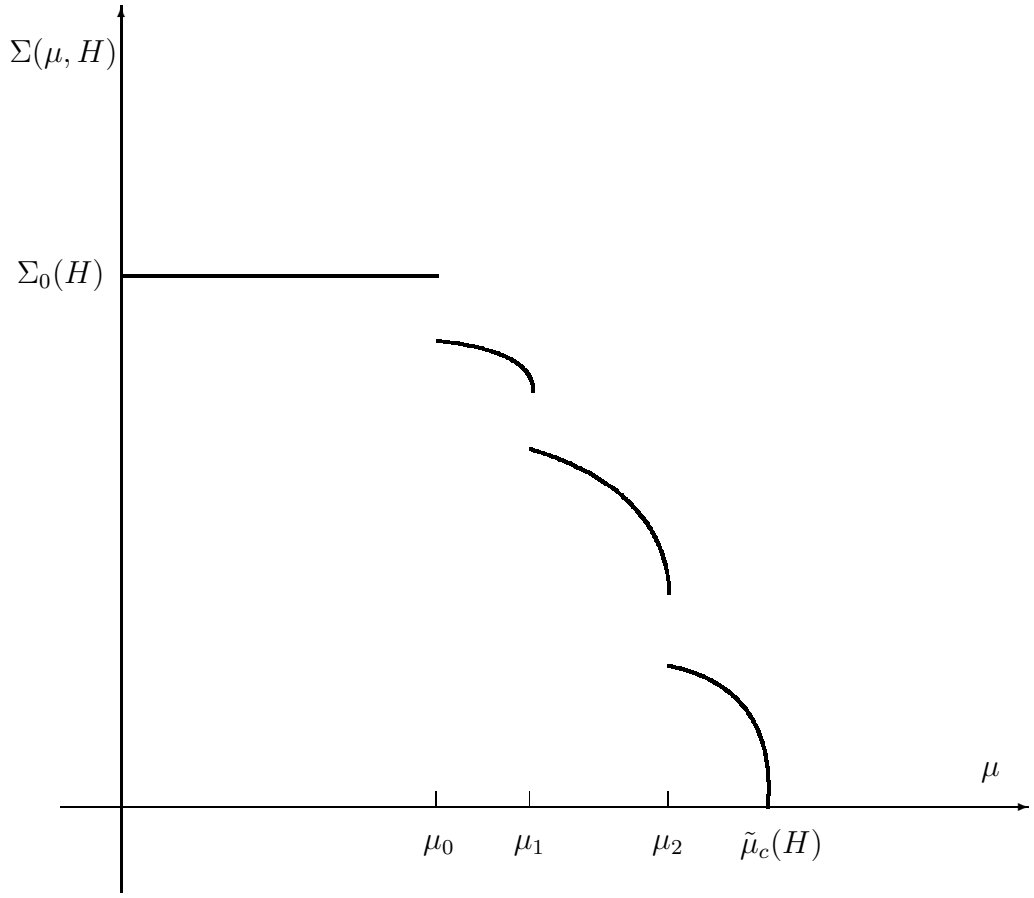

Fig. 7

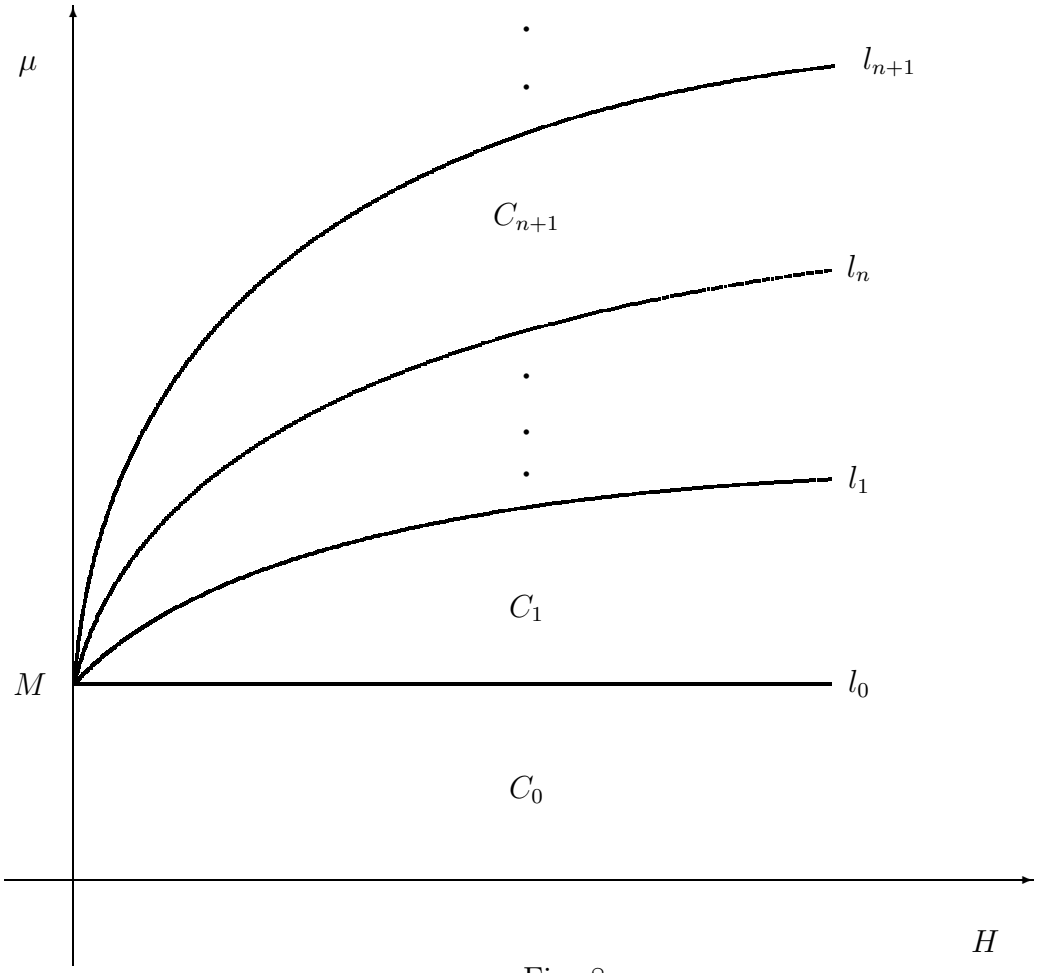

Fig. 8